Electronic Journal of Biotechnology 77 (2025) 66–79

Contents lists available at ScienceDirect

Electronic Journal of Biotechnology

journal homepage: www.elsevier.com/locate/ejbt

Research article

NEDD4L/RHOF axis suppresses the malignant phenotypes and lipid metabolism of breast cancer and NEDD4L is affected by upstream ALKBH5 ☆

Tao Liu, Xiaoming Lin, Rong Liang *

Mammary and Esophageal Department, Affiliated Hospital of Guangdong Medical University, Zhanjiang, China

GRAPHICAL ABSTRACT

NEDD4L/RHOF axis suppresses the malignant phenotypes and lipid metabolism of breast cancer and NEDD4L is affected by upstream ALKBH5

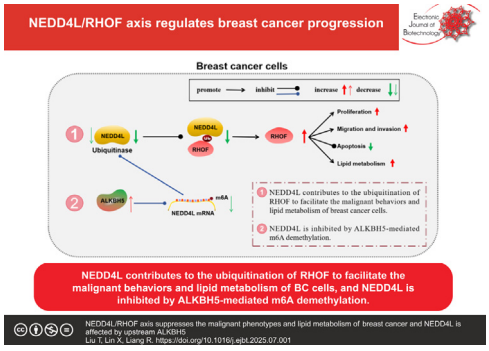

ARTICLE INFO

Article history:
Received 3 April 2025
Accepted 14 July 2025
Available online 13 August 2025

Keywords:
ALKBH5
Breast cancer
Lipid metabolism
Methylation
NEDD4L
RHOF
Suppression malignant phenotypes
Ubiquitination

ABSTRACT

Background: The protein posttranslational modifications, including ubiquitination and methylation, exhibit the essential function in breast cancer. Herein, we aimed to explore the molecular mechanism of neural precursor cell-expressed developmentally downregulated gene 4-like (NEDD4L) associated with Rho GTPase Rif (RHOF) and AlkB homolog 5 (ALKBH5). A series of experiments including expression detection, cell functions, xenograft tumor assay, and interaction analysis was designed.
Results: RHOF was up-regulated in breast cancer samples and cells. Silencing RHOF suppressed breast cancer cell growth, migration, invasion and lipid metabolism. Breast cancer tumorigenesis and lipid metabolism were repressed by RHOF knockdown *in vivo*. NEDD4L impaired RHOF stability by promoting its ubiquitination. NEDD4L overexpression restrained breast cancer cell progression and lipid metabolism via degrading RHOF. ALKBH5 inhibited NEDD4L expression through m6A modification.

☆ Audio abstract available in Supplementary material.
Peer review under responsibility of Pontificia Universidad Católica de Valparaíso.
* Corresponding author.
E-mail address: alenlau4868@163.com (R. Liang).

https://doi.org/10.1016/j.ejbt.2025.07.001

Conclusions: These results evidenced that NEDD4L facilitated the malignant progression of breast cancer via inducing the ubiquitination of RHOF, and NEDD4L was also affected by ALKBH5-mediated m6A demethylation.
How to cite: Liu T, Lin X, Liang R. NEDD4L/RHOF axis suppresses the malignant phenotypes and lipid metabolism of breast cancer and NEDD4L is affected by upstream ALKBH5. Electron J Biotechnol 2025;77. https://doi.org/10.1016/j.ejbt.2025.07.001.

1. Introduction

Breast cancer (BC) is currently the most frequent global malignancy among the women populationand remains the major cause of cancer-associated mortality [1,2]. Latest cancer statistics show that over 2.3 million new cases of BC were diagnosed in 2022, accounting for 11.6% of all cancer cases; and 665,000 deaths occurred, comprising 6.9% of all cancer deaths [3]. BC incidence is increased with age, but there are still some cases at a younger age [4]. BC has different subtypes such as estrogen receptor (ER), progesterone receptor (PR), or human epidermal growth factor receptor 2 (HER2), according to the standard diagnosis by immunohistochemistry (IHC) results [5]. For ER-positive or PR-positive BC, endocrinotherapy, chemotherapy and cyclin-dependent kinases (CDK) 4/6 inhibitors are the main therapies. Target therapy and chemotherapy, antibody-drug conjugates (ADCs) are usually applied for HER2-postive BC [6]. However, drug resistance or toxicity may limit the therapeutic efficacy. BC continues to affect the public health and long-term survival of women [7]. Under the circumstances, awareness of the pathological mechanism of BC malignant development might provide a new clue for the diagnosis and therapies of BC.

Rho GTPase Rif (RHOF) belongs to Rho GTPase family that is implicated in regulating different human malignancies and various biological functions [8]. Rho GTPase signaling can drive cancer initiation and precipitate malignant progression via affecting cancer cell growth, apoptosis and metabolism [9]. RHOF plays an oncogenic role to promote migration, invasion and epithelial mesenchymal transformation in pancreatic cancer [10,11]. RHOF can accelerate the progression of acute myeloid leukemia and increase the chemotherapy resistance [12]. RHOF is aberrantly up-regulated in BC tissues and associated with lymph node metastasis [13]. Nevertheless, the role of RHOF in BC is required to be investigated.

Neural precursor cell-expressed developmentally downregulated gene 4-like (NEDD4L) is an E3 ubiquitin ligase vital to the ubiquitination process, and it is capable of regulating cancer cell functions [14]. NEDD4L suppresses the proliferation and migration abilities of clear cell renal cell carcinoma [15], and it inhibits the malignant phenotypes of esophageal carcinoma through ITGB4 ubiquitination [16]. NEDD4L was evidenced to play an anticancer molecule preventing from the progression of BC [17], and it exhibited the ubiquitination regulation of CD71 in ER-positive BC cells [18]. The potential association between NEDD4L and RHOF is fully unknown. N6-Methyladenosine (m6A) methylation modification is widely present in the modification of mRNA by involving in mRNA processing, maturation, splicing, transport, translation, and degradation, further affecting cellular behaviors of BC [19]. AlkB homolog 5 (ALKBH5) is a m6A demethylase with great importance involved in BC development [20,21]. We have predicted the m6A modification sites in NEDD4L, but it is not clear whether ALKBH5 can trigger m6A modification regulation for NEDD4L in BC.

Dysfunction of lipid metabolism is an all-important metabolic alteration in cancers. Cancer cells can obtain energy and components for biological membranes and signaling molecules through harnessing lipid metabolism, then contributing to cancer cell survival, invasion, and metastasis [22]. NEDD4L has been indicated to promote cellular lipid peroxidation levels in oesophageal squamous cell carcinoma [23], and it can mediate the level of CREB-regulated transcription coactivator 3 (CRTC3), a regulator of lipid metabolism [24]. Thus, it is of great importance to explore the involvement of NEDD4L/RHOF in the lipid metabolism of BC cells.

Currently, this work hypothesized that NEDD4L could affect BC progression and lipid metabolism by regulating RHOF in an ubiquitination-dependent manner. Moreover, ALKBH5 was speculated to affect the m6A modification of NEDD4L.

2. Materials and methods

2.1. Databases

GSE162228 dataset from Gene Expression Omnibus (GEO) database (https://www.ncbi.nlm.nih.gov/geo/query/acc.cgi) was used for expression analysis of RHOF and NEDD4L in BC samples. UALCAN analysis for BC samples from TCGA (https://ualcan.path.uab.edu/cgi-bin/TCGAExResultNew2.pl?genenam=RHOF&ctype=BRCA) was employed to exhibit RHOF expression in different pathological stages of BC. The pancarcinoma analysis of RHOF was indicated by TCGA database (https://www.cancer.gov/ccg/research/genome-sequencing/tcga). Ubibrowser website (https://ubibrowser.bio-it.cn/ubibrowser/) was applied to predict the upstream genes of RHOF. The m6A methylation sites of NEDD4L were predicted through SRAMP (https://www.cuilab.cn/sramp). The binding score of ALKBH5 and NEDD4L was analyzed by RBPsuite (https://www.csbio.sjtu.edu.cn/bioinf/RBPsuite/).

2.2. Patients and samples

A total of 35 individuals were diagnosed as BC and underwent surgical resection without any therapy at the Affiliated Hospital of Guangdong Medical University. Inclusion criteria of patients included: (1) Informed consent of patients or their families; (2) BC was confirmed by pathological or cytological examination; (3) All patients were female; (4) Immunohistochemistry of tissues was HER2-positive or ER-dependent. PR-positive samples have not been included because PR is a target of ER and its expression is dependent on estrogen. ER-positive/PR-positive breast cancer is usually common [25]; (5) Patients with at least one measurable target lesion. Exclusion criteria included: (1) BC patients during pregnancy or lactation (estrogen and progesterone are in an abnormally elevated state); (2) Patients with acute and chronic inflammation (inflammatory changes have certain overlaps with BC results); (3) Patients with liver, kidney and heart dysfunction (the poor overall physical function is difficult to tolerate surgical treatment); (4) Patients with other systemic malignancies (other malignancies may affect BC); (5) Poor compliance of patients. The fresh BC tissues and the corresponding paracancerous tissues were collected during the surgery, then stably stored at −80°C for further detection. Each patient has submitted the informed consent for this study. All procedures involving human samples were in accordance with the Declaration of Helsinki and ratified by the Ethics Committee of Affiliated Hospital of Guangdong Medical University.

2.3. Cell culture and plasmid transfection

SKBR-3 and MCF-7 cells are common cell models for BC research *in vitro* [26,27], and they are not polluted. In addition, SKBR-3 is HER2-positive and MCF-7 is ER-dependent BC cells. Therefore, research of SKBR-3 and MCF-7 cells can provide more extensive evidence for BC. Human normal breast cell line MCF-10A was applied as the normal control group. These cells were all purchased from BioVector NTCC Inc. (Beijing, China). SKBR-3 and MCF-7 cells were cultured with Dulbecco's modified eagle medium (DMEM; Gibco, Carlsbad, CA, USA) including 10% fetal bovine serum (Gibco) and 1% penicillin–streptomycin solution (Gibco) in the incubator with 5% CO_2 at 37°C. MCF-10A cells were cultivated with the specific MEGM medium (Gibco) with the supplement of 100 ng/mL cholera toxin (Sigma, St. Louis, MO, USA) under the same condition. For stable transfection, short hairpin RNA (shRNA) plasmids or pcDNA plasmids were transfected into BC cells through Lipofectamine™ 3000 kit (Invitrogen, Carlsbad, CA, USA). ShRNA targeting RHOF (sh-RHOF), shRNA targeting ALKBH5 (sh-ALKBH5), and shRNA normal control (sh-NC) were bought from GenePharma (Shanghai, China). The pcDNA plasmid (oe-NC), pcDNA-NEDD4L (oe-NEDD4L), pcDNA-RHOF (oe-RHOF) were constructed by RIBOBIO (Guangzhou, China).

2.4. Real-time quantitative polymerase chain reaction (RT-qPCR)

Firstly, total RNA extraction from human samples and cells was carried out using Trizol (Sangon, Shanghai, China). Subsequently, total RNA was transcribed to obtain cDNA through First Strand cDNA Synthesis Master Mix (Sangon). Then, cDNA was amplified by SYBR Green PCR Master Mix (Ambion, Carlsbad, CA, USA) utilizing the specific primers (Table 1). All operations were implemented according to the manufacturers' instruction books. Eventually, gene expression was analyzed via the $2^{-\Delta\Delta Ct}$ method.

2.5. Western blot

Radioimmunoprecipitation assay (RIPA) buffer (Thermo Fisher Scientific, Waltham, MA, USA) was applied for the extraction of protein samples from tissues and cells. A total of 50 μg proteins of each sample were separated by 10% sodium dodecyl sulfate–polyacrylamide gel electrophoresis (SDS-PAGE) and transferred to polyvinylidene fluoride (PVDF) membranes (Thermo Fisher Scientific). To prevent the non-specific protein binding, the membranes were sealed in blocking solution (Sangon). Then, the incubation (1:1000) of the primary antibodies (Abcam, Cambridge, UK) targeting RHOF (ab101349), NEDD4L (ab46521), ALKBH5 (ab195377), B-cell lymphoma-2 (Bcl-2; ab182858), Bcl-2-associated X (Bax; ab32503), Fatty Acid Synthase (FASN; ab128870), sterol regulatory element-binding protein 1 (SREBP1; ab28481) was performed at 4°C overnight. These gene levels were normalized by β-actin (ab8227, 1:2000). Then, the secondary antibody (Abcam, ab205718, 1:2000) was incubated at room temperature for 1 h. ECL Substrate Kit (Abcam) was utilized for the appearance of protein blots, and the signals were analyzed by Image J software.

Table 1
Primer sequences used for RT-qPCR.

Name	Primers for PCR (5′-3′)	
RHOF	Forward	CTCTTGGCTCCGCTAGTGC
	Reverse	AGGTTCAGGGTCACCTCCTT
NEDD4L	Forward	CTCCTGTGACCTTGTCACCC
	Reverse	ACGGATCACTGGCTCCAAAG
ALKBH5	Forward	TGCAAGCTCATGCAAACACC
	Reverse	GACCCAACGTGGCAAGTCTA
β-actin	Forward	GGATTCCTATGTGGGCGACGA
	Reverse	GCGTACAGGGATAGCACAGC

2.6. Cell Counting Kit-8 (CCK-8) assay

Cell viability was detected by CCK-8 assay. SKBR-3 and MCF-7 cells were cultured for 24 h, followed by transfection with plasmids for different times (20 h, 40 h, 60 h, or 80 h). Then, the cell medium was discarded, and cells were added with 10 μL/well CCK-8 solution (Sangon). The absorbance at 450 nm was examined under the microplate reader.

2.7. Ethynyl-2′-deoxyuridine (EdU) assay

Transfected cells were seeded into the 96-well plate with 5000 cells/well for 48 h, and then EdU detection was performed by EdU Imaging Detection Kit (Sangon). Briefly, cells were added with 300 μL 1 × EdU medium for 2 h to label the DNA. After cells were fixed with 4% paraformaldehyde (Sangon) and infiltrated with Triton X-100 solution (Sangon), cells were treated with 100 μL EdU detection solution for 30 min. Then, nuclei were stained with diamidine phenylindole (DAPI; Sangon) for 20 min, and cell detection was performed under a fluorescence microscope (Olympus, Tokyo, Japan). Cell proliferation was assessed by EdU-positive (EdU + DAPI) cells.

2.8. Transwell assay

Cell migration and invasion were examined using a transwell chamber (8 μm pore size of filter membranes, Corning Inc., Corning, NY, USA). For migration, the upper chamber was seeded with 1×10^5 SKBR-3 and MCF-7 cells resuspended in serum-free medium and complete medium was added into the lower chamber. After incubation for 24 h, migrated cells were fixed with 4% paraformaldehyde (Sangon) for 30 min and stained with 0.1% crystal violet (Sangon) for 30 min. For invasion, 50 μL of matrigel (Corning Inc.) diluted in serum-free medium was precoated to the upper transwell chamber at 37°C for 4 h. To ensure the uniform coating, the bottom of the upper chamber was completely covered with matrigel with no air bubbles. The subsequent procedures were in accordance with the detection of migration. Images of cells were observed through the inverted microscope (Olympus), and then, migrated and invaded cells were numbered.

2.9. Flow cytometry

Cell apoptosis was measured using the Annexin V-FITC Apoptosis Detection Kit (Sigma). BC cells after transfection were added with Annexin V-FITC and Propidium Iodide (PI) as per the supplied specification. Cell condition was determined via a BD Accuri C6 flow cytometer (BD Biosciences, San Diego, CA, USA). Apoptotic cells were analyzed using the BD Accuri C6 system (32-bit) software (BD Biosciences). Annexin V+/PI- and Annexin V+/PI+ stained cells were regarded as the apoptotic cells.

2.10. Triglyceride, cholesterol and phospholipid detection

After transfection, cells were lysed with RIPA buffer for 45 min. Cell homogenates were acquired using chloroform and methanol solution (chloroform: methanol = 2:1), followed by the extraction of lipid. The levels of triglyceride, cholesterol, and phospholipid were respectively measured via Triglyceride Quantification Kit, Cholesterol Quantification Assay kit and Phospholipid Quantification Kit (Sigma) under the microplate reader (Thermo Fisher Scientific), in strict line with the users' guidelines.

2.11. Tumor xenograft assay

This animal assay was authorized by the Animal Ethical Committee of Affiliated Hospital of Guangdong Medical University. All operations on mice were performed in line with the relevant guidelines and regulations of Care and Use of Laboratory Animals published by the National Institutes of Health (NIH). Six-week-old BALB/c female nude mice (Vital River, Beijing, China) were divided into two groups with 5 mice of each group. The stably transfected MCF-7 cells with sh-NC or sh-RHOF were subcutaneously injected into the flank of mice, with 2×10^6 cells of each mouse. Tumor volume (length × width^2/2) was recorded every 5 d. All mice were euthanized by using the flow rate of CO_2 to displace the 30% air of cage each minute according to the current guideline of the American Veterinary Medical Association (AVMA) after 25 d, and tumors were photographed. The maximal tumor diameter permitted by the ethics committee was approximately 15 mm, and our maximal tumor diameter was not exceeded. The protein levels of caspase-3, cleaved caspase-3 and RHOF were detected by IHC analysis. The mRNA levels of FASN and SREBP1 in tumors from mice were examined to assess lipid metabolism.

2.12. Glutathione S-transferase (GST) pull-down assay

GST fusion proteins were prepared according to the standard protocol. Briefly, NEDD4L or RHOF cDNA sequence was synthesized and subcloned to construct the GST-NEDD4L and GST-RHOF plasmids, which were then expressed in the *E. coli* BL21. Then, GST-NEDD4L or GST-RHOF fusion proteins were purified using glutathione agarose beads (Thermo Fisher Scientific). Then, the pure GST-NEDD4L or GST-RHOF protein was incubated with cell lysates from HEK293T cells overexpressing RHOF or NEDD4L at 4°C overnight. GST protein binding to glutathione agarose was used as a negative control. After washing with binding buffer, the bound proteins were eluted for western blot detection of RHOF and NEDD4L.

2.13. Co-immunoprecipitation (Co-IP) assay

Cell lysates were prepared from SKBR-3 and MCF-7 using RIPA buffer (Thermo Fisher Scientific) and then incubated with anti-RHOF/anti-NEDD4L/anti-IgG and Protein A/G Magnetic Beads (Pierce, Rockford, IL, USA). Afterwards, the protein–protein complexes were washed with 0.5% PBS-Triton X-100 and resuspended with SDS-PAGE protein loading buffer for western blot analysis of RHOF and NEDD4L.

2.14. RHOF protein stability testing

The protein stability of RHOF was examined through cycloheximide (CHX) treatment. SKBR-3 and MCF-7 cells were transfected with oe-NC or oe-NEDD4L, followed by incubation with 100 μM CHX (Sigma). Cells were harvested at different times (0 h, 3 h, 6 h, 9 h and 12 h) for western blot detection of RHOF.

2.15. Ubiquitination assay

HEK293T cells were transfected with oe-NC/oe-NEDD4L, and then, cell lysates were incubated with anti-RHOF and protein A/G agarose beads (Beyotime). Then, the immunoprecipitated proteins were obtained for western blot detection of UB and RHOF.

2.16. NEDD4L mRNA stability assay

SKBR-3 and MCF-7 cells were transfected with sh-NC or sh-ALKBH5 for 24 h; then, the cell culture medium was treated with 2 mg/mL Actinomycin D (Sigma) for 0 h, 3 h, 6 h, 9 h, or 12 h. Then, total RNA was extracted, and NEDD4L mRNA detection was performed using RT-qPCR.

2.17. RNA immunoprecipitation (RIP) assay

The interaction between ALKBH5 and NEDD4L was examined using Magna RIP RNA-Binding Protein Immunoprecipitation Kit (Millipore, Billerica, MA, USA). SKBR-3 and MCF-7 cells were lysed in RIP lysis Buffer and then incubated with anti-ALKBH5 or anti-IgG-coated Protein A magnetic beads at 4°C overnight. The proteinase K was added to remove proteins, and the immunoprecipitated RNA was used for mRNA detection of NEDD4L by RT-qPCR.

2.18. Methylated RNA Immunoprecipitation (MeRIP)

Total RNA was extracted from cells after transfection with sh-NC or sh-ALKBH5, followed by treatment with DNase (Sigma) to remove the genomic DNA. Then, the fragments were incubated with anti-m6A or rabbit IgG through a Magna MeRIP™ m6A kit (Millipore). Then mRNA level of NEDD4L was determined via RT-qPCR.

2.19. Statistical analysis

Assays were implemented for three independent times with three parallels of each time. Data were then manifested as the mean ± standard deviation (SD), followed by data analysis through SPSS and GraphPad Prism. For statistical difference, Student's *t*-test was used for difference analysis between two groups, and analysis of variance (ANOVA) followed by Tukey's test was applied for that among multiple groups. In terms of the statistical level, the difference was significant if $p < 0.05$.

3. Results

3.1. RHOF was highly expressed in BC samples and cells

Firstly, the aberrant expression of RHOF was discovered by online databases. GSE162228 dataset has indicated RHOF as an up-regulated gene in BC tissues (Fig. 1A). Meanwhile, UALCAN database analysis for TCGA samples demonstrated that RHOF expression was higher in different pathological stages of BC by comparison with normal patients (Fig. 1B). Then, we performed RT-qPCR and western blot to examine whether RHOF expression was consistent with the databases. The results revealed that RHOF mRNA and protein levels were significantly increased in BC tissues contrasted to normal controls (Fig. 1C–D). Likewise, SKBR-3 and MCF-7 cells revealed the high expression of RHOF relative to MCF-10A cells (Fig. 1E–F). Additionally, expression of RHOF across TCGA cancers exhibited a high tendency of RHOF in BC (Fig. 1G). Our analysis confirmed RHOF upregulation in BC.

3.2. RHOF knockdown restrained BC cell malignant phenotypes

The abnormal upregulation of RHOF implied its potential involvement in BC progression, and then, we performed loss-of-function assays to affirm it. Knockdown efficiency of shRNA was examined by western blot, and the results showed that RHOF protein level was evidently decreased in SKBR-3 and MCF-7 cells with transfection of sh-RHOF (Fig. 2A). CCK-8 and EdU assays were used to assess cell growth. Silence of RHOF significantly reduced cell viability (Fig. 2B) and EdU positive cells (Fig. 2C).

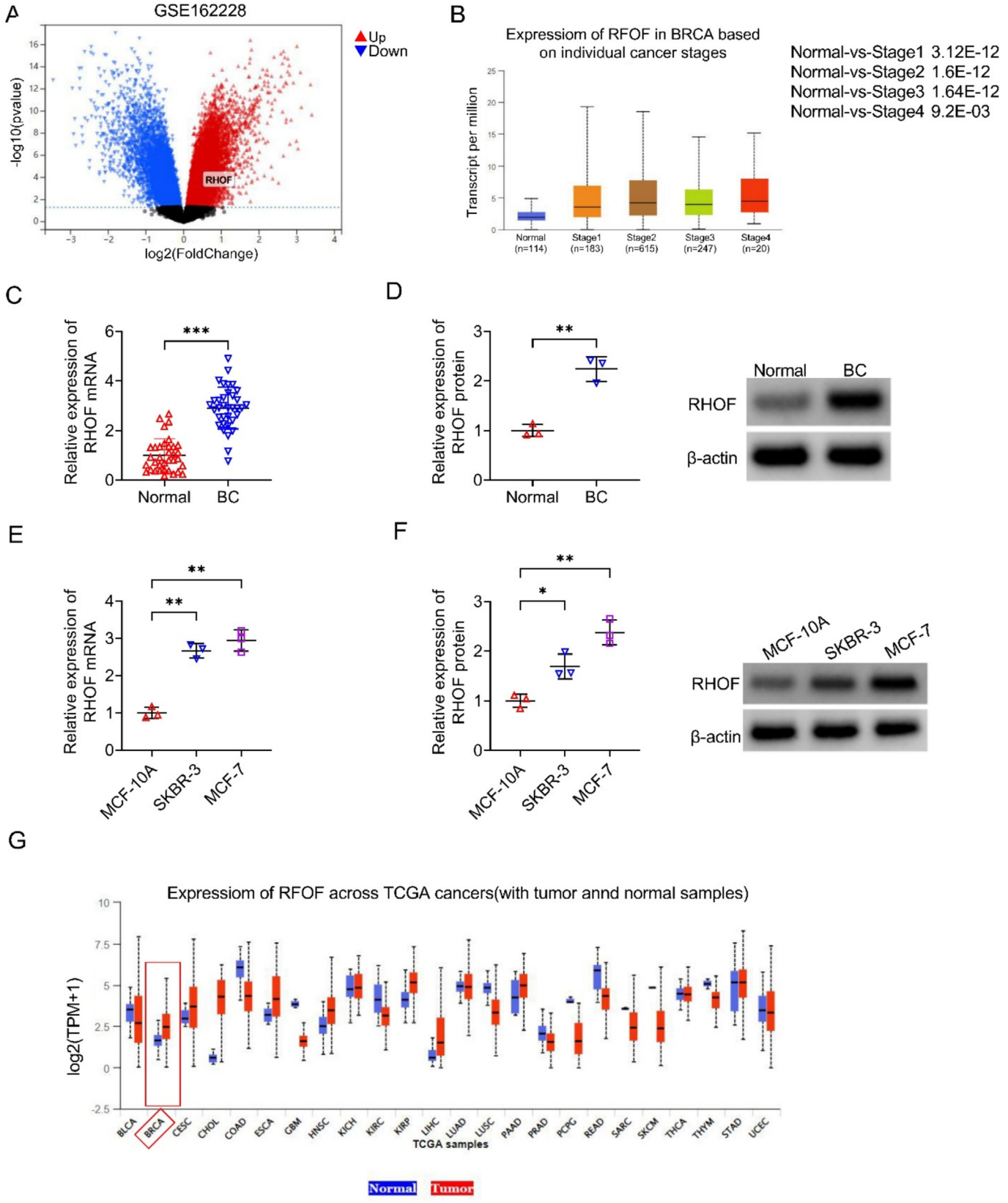

Fig. 1. RHOF was highly expressed in BC samples and cells. (A) RHOF expression in BC by GSE162228 dataset. (B) RHOF expression in different pathogenic stages of BC by TCGA-BRCA database. (C–F) RHOF mRNA and protein levels in BC samples (C–D) and SKBR-3, MCF-7 cells (E-F) were examined by RT-qPCR and western blot. (G) Expression of RHOF in BC of TCGA cancers. Detection experiments were performed by three biological repetitions. $^{*}p < 0.05$, $^{**}p < 0.01$, $^{***}p < 0.001$.

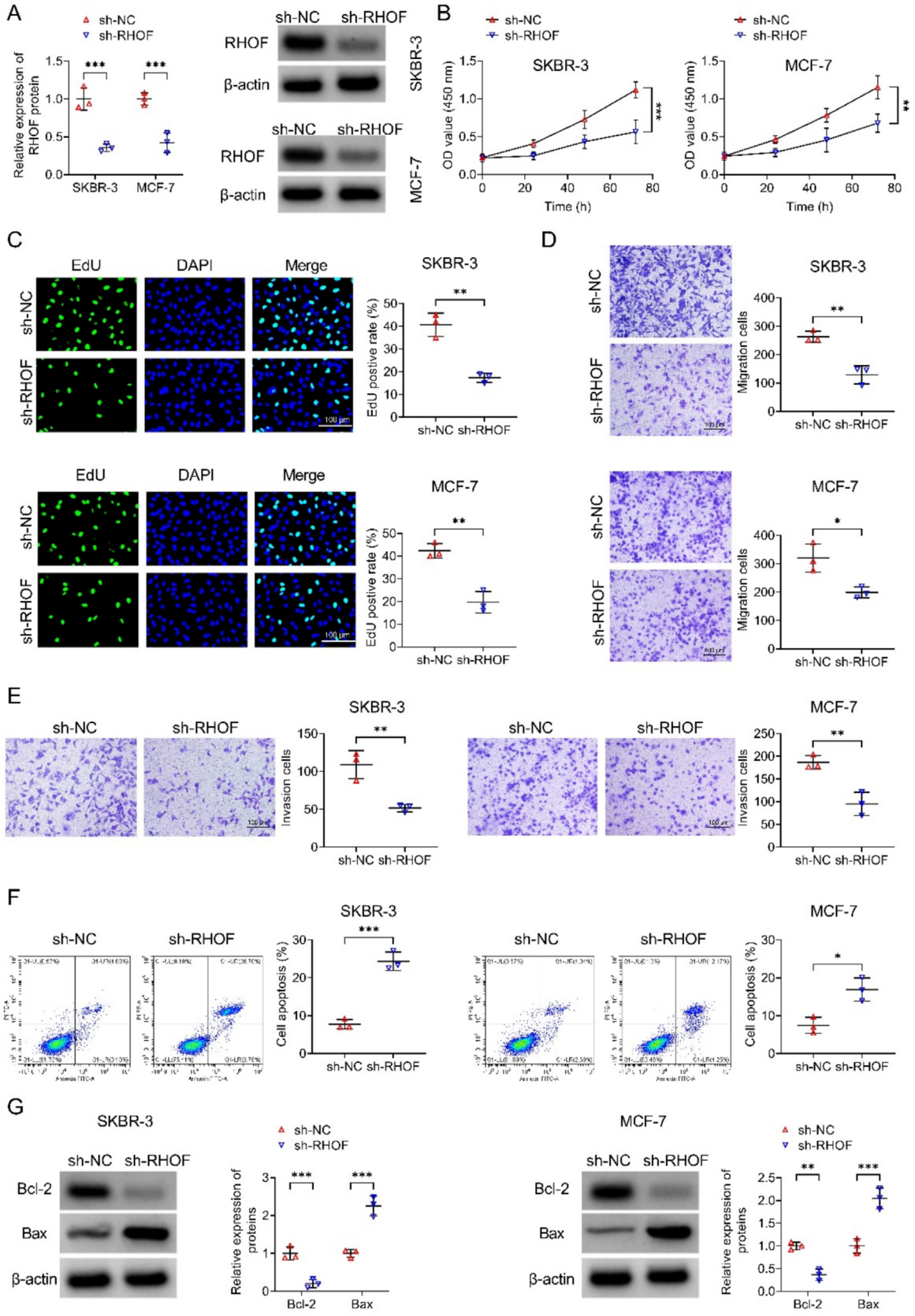

Fig. 2. RHOF knockdown restrained BC cell malignant phenotypes. SKBR-3 and MCF-7 cells were divided into sh-NC and sh-RHOF groups. (A) Knockdown efficiency of sh-RHOF was assessed using western blot. (B) Cell viability was determined using CCK-8 assay. (C) Cell proliferation was evaluated via EdU assay. (D–E) Abilities of migration (D) and invasion (E) were measured by transwell assay. (F) Cell apoptosis detection was carried out by flow cytometry. (G) Bcl-2 and Bax protein levels were analyzed via western blot. Detection experiments were performed by three biological repetitions. $^{*}p < 0.05$, $^{**}p < 0.01$, $^{***}p < 0.001$.

RHOF downregulation suppressed cell migration (Fig. 2D) and invasion (Fig. 2E) according to the transwell assay. For cell apoptosis, flow cytometry demonstrated a promoting effect of RHOF knockdown on the percentage of apoptotic cells (Fig. 2F). In addition, RHOF expression reduction inhibited protein expression of anti-apoptotic Bcl-2 and up-regulated pro-apoptotic Bax in SKBR-3 and MCF-7 cells (Fig. 2G). Collectively, our results suggested that RHOF inhibition hindered the malignant development of BC cells.

3.3. Silencing RHOF suppressed lipid metabolism in BC cells

Given the impact of RHOF on BC cell malignant phenotypes, and considering its potential links to cellular metabolism, we next investigated its role in lipid metabolism. Triglyceride, cholesterol, and phospholipid are common lipids involved in the lipid metabolism. The levels of triglyceride (Fig. 3A), cholesterol (Fig. 3B) and phospholipids (Fig. 3C) were all much lower in sh-RHOF group than those in sh-NC group of SKBR-3 and MCF-7 cells. These results demonstrated that RHOF deficiency repressed lipid formation in BC cells. FASN and SREBP1 function as central regulators of lipid metabolism [28]. Transfection of sh-RHOF caused the significant protein inhibition of FASN and SREBP1, compared with transfection of sh-NC (Fig. 3D–E). Thus, lipid metabolism was constrained in BC cells with the silence of RHOF.

3.4. RHOF promoted BC tumor growth and lipid metabolism in vivo

After affirming the role of RHOF *in vitro*, we further explored RHOF function *in vivo* by establishing a xenograft model to better elucidate the implication of RHOF in BC. Tumor volume (Fig. 4A) was obviously declined in xenograft model of sh-RHOF group, by comparison with sh-NC group. Tumor images were shown in Fig. 4B. IHC analysis indicated that protein levels of caspase-3 and cleaved caspase-3 (apoptotic markers) were up-regulated, and RHOF protein level was reduced in sh-RHOF group relative to sh-NC group (Fig. 4C). In addition, it was observed that RHOF downregulation suppressed the mRNA levels of FASN and SREBP1, indicating that RHOF facilitated lipid metabolism in mice (Fig. 4D–E). These results suggested the promoting effects of RHOF on BC tumorigenesis and lipid metabolism *in vivo*.

3.5. NEDD4L interacted with RHOF to promote its ubiquitination

On the premise that the functions of RHOF have been confirmed, it is important to explore the molecular mechanism associated with RHOF. The upstream genes of RHOF were predicted by Ubibrowser website, and NEDD4L was one of the targets in the upstream of RHOF (Fig. 5A). Regarding the expression of NEDD4L, GSE162228 dataset identified NEDD4L as a down-regulated gene in BC (Fig. 5B). In our BC tissues, NEDD4L was also expressed with

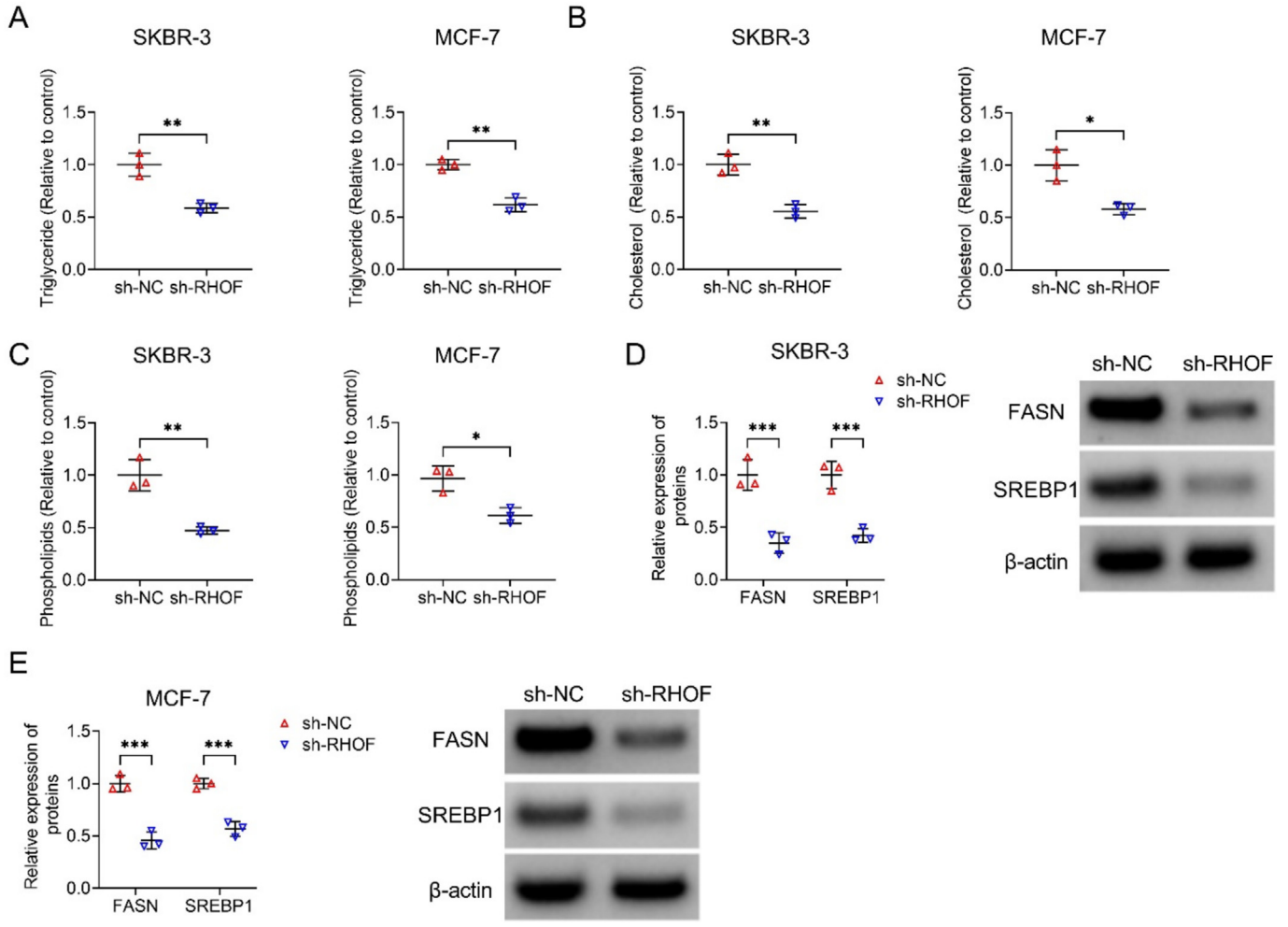

Fig. 3. Silencing RHOF suppressed lipid metabolism in BC cells. SKBR-3 and MCF-7 cells were transfected with sh-NC and sh-RHOF, respectively. (A–C) Examination of triglyceride (A), cholesterol (B) and phospholipids (C) was implemented using the corresponding commercial kits. (D-E) Western blot was performed for protein detection of FASN and SREBP1. Detection experiments were performed by three biological repetitions. $^{*}p < 0.05$, $^{**}p < 0.01$, $^{***}p < 0.001$.

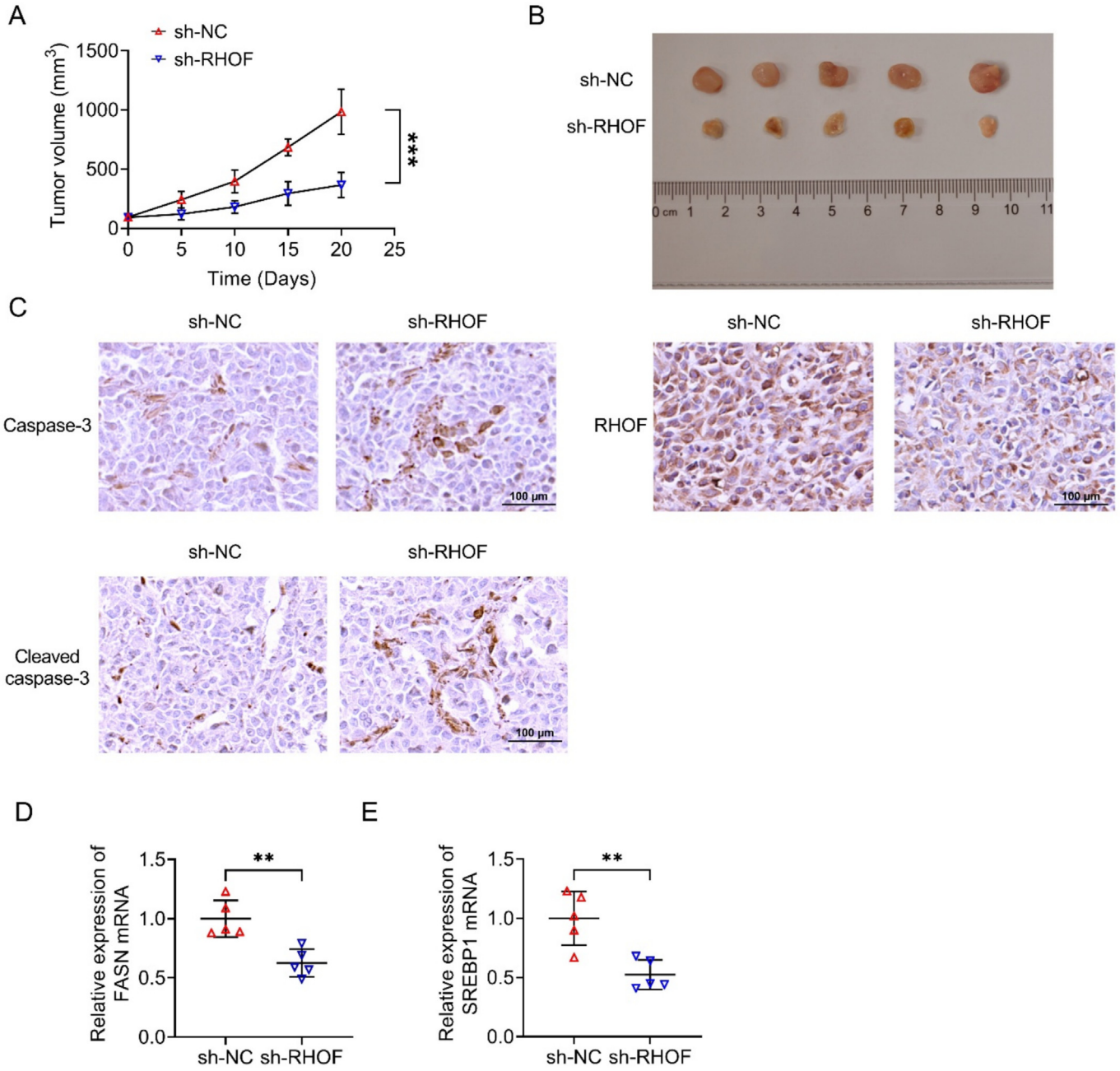

Fig. 4. RHOF promoted BC tumor growth and lipid metabolism *in vivo*. (A) Tumor volume in sh-NC and sh-RHOF models. (B) Tumor images and scale. (C) IHC analysis for protein levels of caspase-3, cleaved caspase-3 and RHOF. (D–E) FASN and SREBP1 mRNA levels in tumor tissues. Detection experiments were performed by three biological repetitions. $^{**}p < 0.01$, $^{***}p < 0.001$.

a low level through the detection of RT-qPCR and western blot (Fig. 5C–D). Similarly, NEDD4L mRNA and protein levels were prominently decreased in SKBR-3 and MCF-7 cells (Fig. 5E–F). Further assays were carried out to validate whether NEDD4L interacted with RHOF. GST pull-down test manifested that RHOF was pulled down by GST-NEDD4L protein and NEDD4L was also pulled down by GST-RHOF protein (Fig. 5G). By performing Co-IP, the interaction between NEDD4L and RHOF was further confirmed in SKBR-3 and MCF-7 cells (Fig. 5H–I). Subsequently, CHX treatment was performed to examine the protein stability of RHOF. As shown in Fig. 5J–K, overexpression of NEDD4L limited the protein stability of RHOF under the treatment of CHX. Moreover, NEDD4L upregulation enhanced the ubiquitination level of RHOF in BC cells (Fig. 5L). Taken together, NEDD4L reduced RHOF level by arousing the ubiquitination of RHOF.

3.6. RHOF overexpression rescued the effects of NEDD4L on BC cells

Given the target binding between NEDD4L and RHOF, we speculated that the regulation of NEDD4L in BC progression was related to RHOF. The regulatory network between NEDD4L and RHOF was investigated in BC cells via a series of reverted experiments. Analysis of western blot manifested that co-transfection with oe-RHOF reversed oe-NEDD4L-inhibited RHOF level, suggesting the excellent overexpression efficiency of oe-RHOF (Fig. 6A). Overexpression of NEDD4L repressed cell viability (Fig. 6B) and proliferation

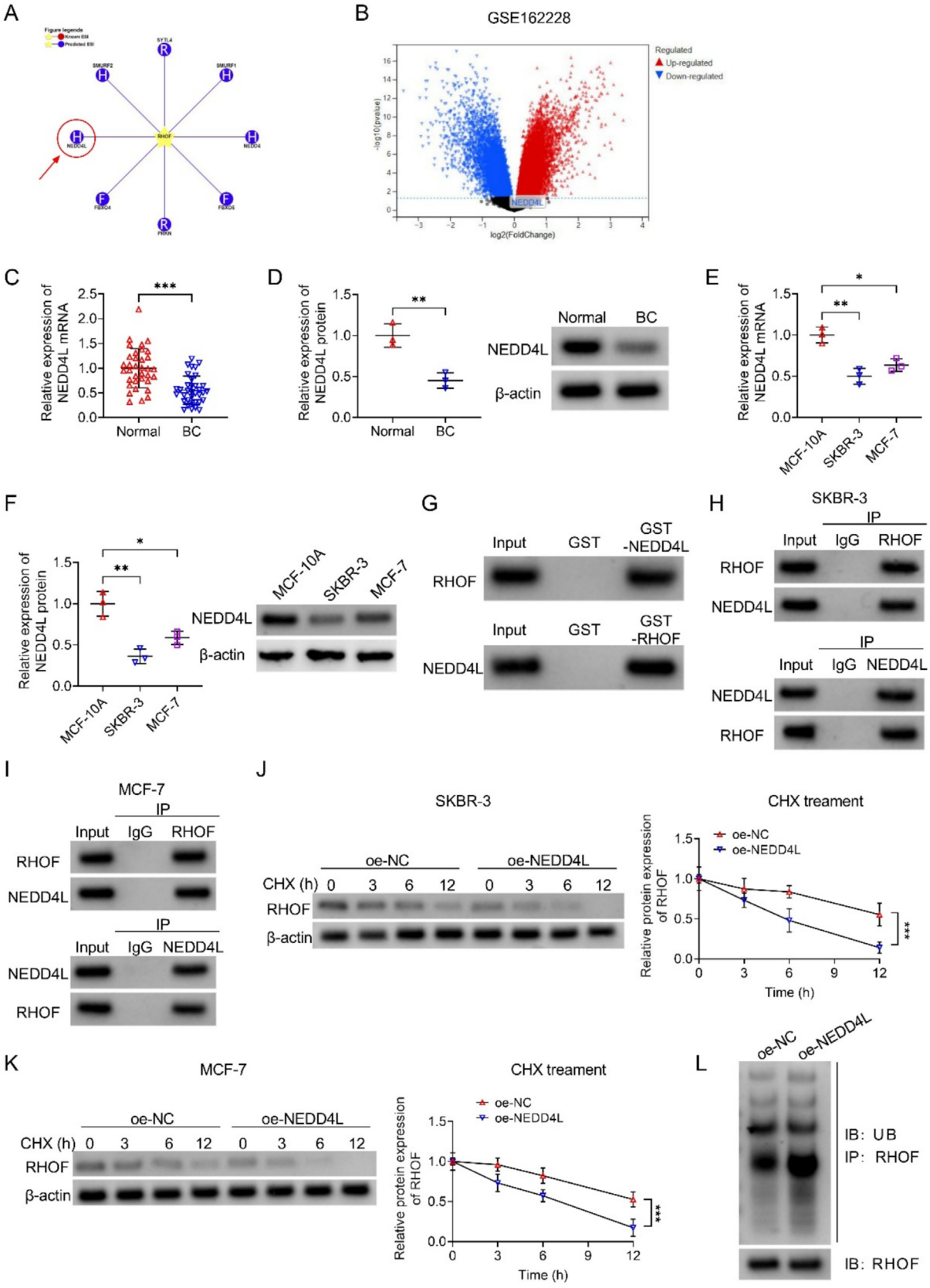

Fig. 5. NEDD4L interacted with RHOF to promote its ubiquitination. (A) NEDD4L was predicted as an upstream gene of RHOF by Ubibrowser website. (B) The expression of NEDD4L in GSE162228 dataset. (C-F) NEDD4L mRNA and protein detection by RT-qPCR and western blot in BC tissues (C–D) and cells (E–F). (G–I) GST pull-down (G) and Co-IP (H–I) were performed to analyze the interaction between NEDD4L and RHOF. (J–K) RHOF stability after NEDD4L overexpression was detected by western blot under CHX treatment. (L) The effect of NEDD4L overexpression on the ubiquitination level of RHOF. Detection experiments were performed by three biological repetitions. $^{*}p < 0.05$, $^{**}p < 0.01$, $^{***}p < 0.001$.

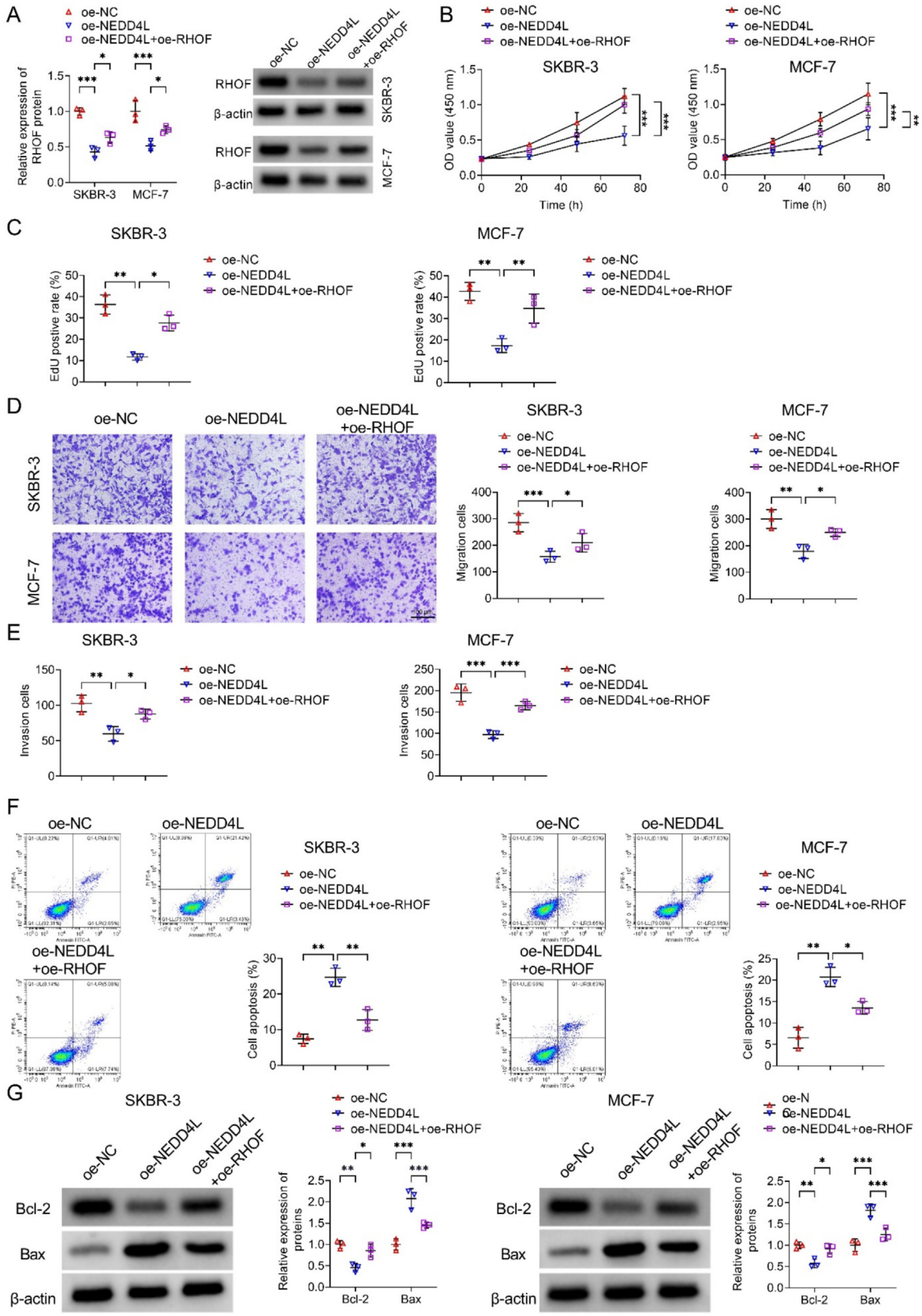

Fig. 6. RHOF overexpression rescued the effects of NEDD4L on BC cells. SKBR-3 and MCF-7 cells were treated with oe-NC, oe-NEDD4L, or oe-NEDD4L + oe-RHOF. (A) Western blot for protein detection of RHOF. (B) CCK-8 assay for cell viability. (C) EdU assay for cell proliferation. (D–E) Transwell assay for assessment of migration (D) and invasion (E). (F) Flow cytometry for cell apoptosis. (G) Western blot for detection of apoptotic markers. Detection experiments were performed by three biological repetitions. $^{*}p < 0.05$, $^{**}p < 0.01$, $^{***}p < 0.001$.

(Fig. 6C), followed by the restoration after upregulation of RHOF. Cells with migration (Fig. 6D) and invasion (Fig. 6E) were decreased by oe-NEDD4L, whereas oe-RHOF overturned these impacts. Meanwhile, RHOF overexpression recuperated the increase of apoptotic cells (Fig. 6F) and the changes of apoptotic markers (Fig. 6G) caused by oe-NEDD4L. In combination with these results, we considered that the anti-cancer function of NEDD4L in BC cells was achieved by downregulating RHOF.

3.7. NEDD4L impeded lipid metabolism in BC cells by mediating RHOF

The interaction between NEDD4L and RHOF has been validated in regulating malignant phenotypes; then, the effect of NEDD4L/RHOF on lipid metabolism was further studied. Transfection of oe-NEDD4L inhibited levels of triglyceride (Fig. 7A), cholesterol (Fig. 7B) and phospholipids (Fig. 7C); then, the overexpression of RHOF eliminated these changes. After RHOF expression was enhanced, oe-NEDD4L-mediated protein inhibition of FASN and SREBP1 was ameliorated by a significant level (Fig. 7D–E). All in all, lipid metabolism in BC cells was impaired by NEDD4L through the level reduction of RHOF.

3.8. ALKBH5 inhibited mRNA stability of NEDD4L by m6A modification

RHOF has been verified as a downstream target of NEDD4L, but the upstream targets associated with NEDD4L remain unclear. SRAMP website predicted that NEDD4L had multiple m6A methylation modification sites (Fig. 8A), which implied that NEDD4L might participate in the m6A modification. Subsequently, RBPsuite website indicated the binding between ALKBH5 and NEDD4L (Fig. 8B). Thus, we hypothesized that there was the m6A modification between ALKBH5 and NEDD4L. Expression analysis by RT-qPCR and western blot identified that ALKBH5 was highly expressed in BC samples (Fig. 8C) and cells (Fig. 8D). Knockdown of ALKBH5 promoted NEDD4L protein level in SKBR-3 and MCF-7 cells, suggesting the negative regulation of ALKBH5 on NEDD4L expression (Fig. 8E). After actinomycin D treatment, silence of ALKBH5 enhanced the stability of NEDD4L in BC cells (Fig. 8F–G). RIP assay affirmed the high enrichment of NEDD4L by anti-ALKBH5 in SKBR-3 and MCF-7 cells (Fig. 8H–I). Further MeRIP analysis testified that the m6A level of NEDD4L was distinctly increased after ALKBH5 expression was knocked down (Fig. 8J–K), suggesting that ALKBH5 induced demethylation of NEDD4L

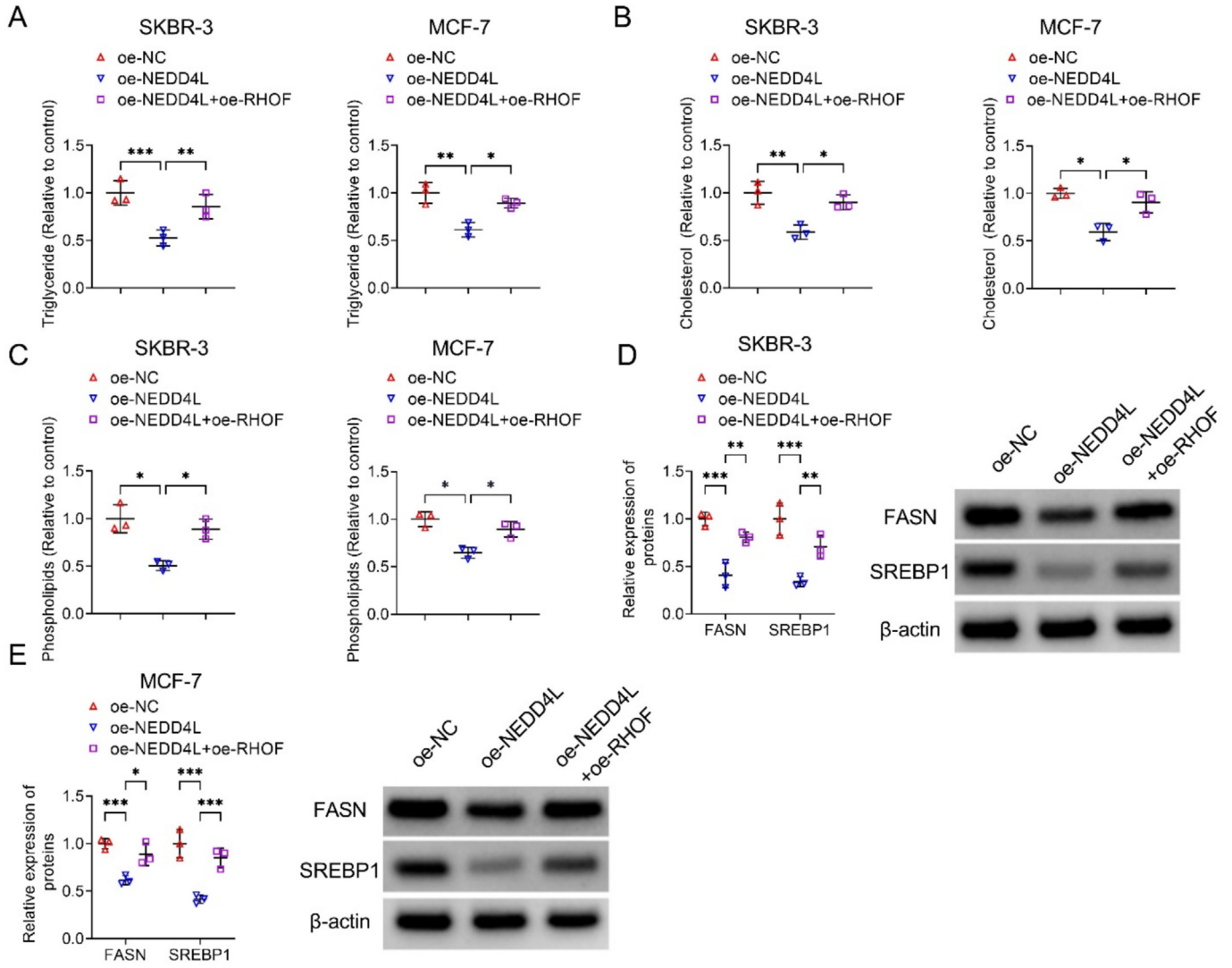

Fig. 7. NEDD4L impeded lipid metabolism in BC cells by mediating RHOF. Transfection with oe-NC, oe-NEDD4L, or oe-NEDD4L + oe-RHOF was performed in SKBR-3 and MCF-7 cells. (A–C) Triglyceride (A), cholesterol (B) and phospholipids (C) were determined through the corresponding commercial kits. (D–E) FASN and SREBP1 protein levels were tested using western blot. Detection experiments were performed by three biological repetitions. $^{*}p < 0.05$, $^{**}p < 0.01$, $^{***}p < 0.001$.

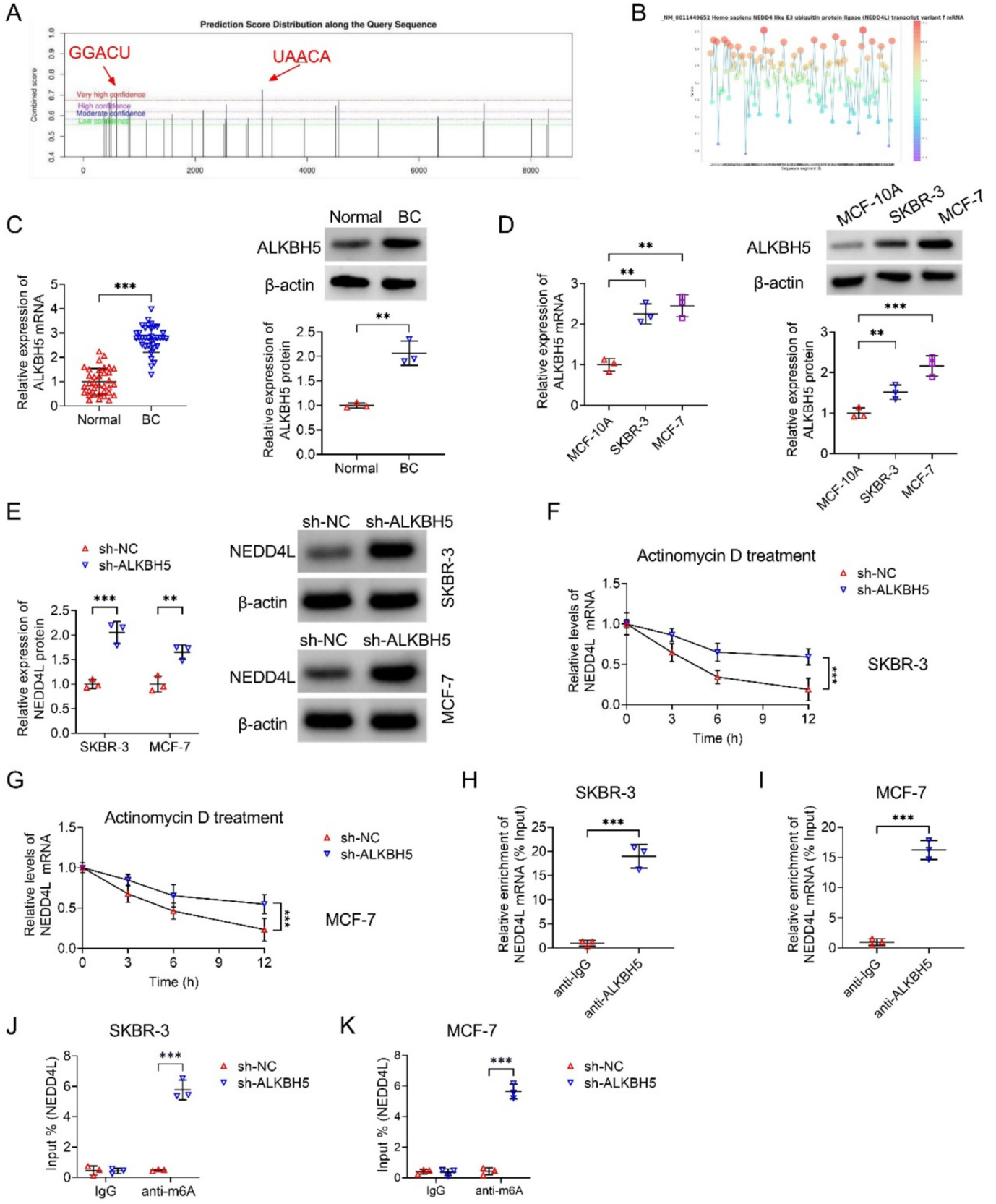

Fig. 8. ALKBH5 inhibited mRNA stability of NEDD4L by m6A modification. (A) SRAMP website predicted the m6A methylation sites of NEDD4L. (B) The binding between ALKBH5 and NEDD4L in RBPsuite website. (C–D) RT-qPCR and western blot analysis for ALKBH5 mRNA and protein expression in BC tissues (C) and cells (D). (E) NEDD4L protein detection was performed by western blot in BC cells transfected with sh-NC or sh-ALKBH5. (F–G) NEDD4L mRNA stability was assessed by RT-qPCR after sh-NC or sh-ALKBH5 transfection and actinomycin D treatment. (H-I) RIP was conducted to explore the interaction between ALKBH5 and NEDD4L. (J-K) The m6A level of NEDD4L after knockdown of ALKBH5 was assessed by MeRIP assay. Detection experiments were performed by three biological repetitions. $^{**}p < 0.01$, $^{***}p < 0.001$.

mRNA. Hence, ALKBH5 reduced NEDD4L expression via the m6A modification for NEDD4L. The hypothesis about the m6A modification between ALKBH5 and NEDD4L was affirmed.

4. Discussion

As one of the commonest malignant cancers in women, BC has serious impacts on patients' physical and psychological health. It is becoming urgent and important to probe into the molecular mechanism underlying the occurrence and development of BC. Herein, we mainly certified the oncogenic function of RHOF in BC and its ubiquitination regulation by NEDD4L.

Aberrant expression of gene has implied the potential function in cancer progression. RHOF was certified to be aberrantly overexpressed in pancreatic cancer, and it expedited cell motility and glycolysis [10]. Similarly, dysregulation of RHOF was important for promoting esophageal inflammation that further mediated esophageal squamous cell cancer [29]. In BC, we affirmed the abnormal upregulation of RHOF through online analysis and expression detection in tissues or cells. Subsequently, loss-of-function assays were conducted for the function exploration of RHOF in BC. Cell development including proliferation, invasion or migration was constrained, while apoptosis was accelerated after knocking down RHOF in BC cells. Therefore, RHOF acted as an oncogene to promote the progression of BC cells. In addition, metabolism alteration is considered as one of the hallmarks of human cancers. Among metabolisms, lipid metabolism is significant to support tumorigenesis and progression by promoting lipid synthesis and providing energy [22,30]. As such, targeting lipid metabolism is great potential for anti-cancer therapies [31]. Triglyceride, cholesterol and phospholipid are the main lipids in lipid metabolism. Activated adipocytes by cancer cells can lead to the lipolysis of the stored triglyceride, and the secreted fatty acids are subsequently delivered to cancer cells for uptake [32]. Cholesterol is one of the key components of biological membranes, and the abnormal accumulation of cholesterol can affect signal transduction events at the membrane by motivating the malignant cellular behaviors [33]. In addition, phospholipid peroxidation drives iron-dependent ferroptosis, which is associated with cancer progression at every stage [34]. Thus, it is of great significance to assess the lipids. Through the detection by kits, we observed that RHOF knockdown evoked the suppression of triglyceride, cholesterol and phospholipid, which testifies the promotion of lipid metabolism by RHOF in BC cells. FASN serves as a central modulator of lipid metabolism, ultimately affecting cancer cell growth and survival [35]. The previous study has demonstrated that FASN disruption triggered brain metastasis of BC [36]. Our protein detection for FASN showed that it was down-regulated by the silence of RHOF, which further suggested the promoting effect of RHOF on lipid metabolism. SREBP1 is a key transcription factor controlling cholesterol biosynthesis, lipid homeostasis, and fatty acid synthesis in lipid metabolism [37]. RHOF downregulation-mediated expression inhibition of SREBP1 also manifested that RHOF contributed to lipid metabolism to support BC cell progression. Moreover, RHOF also enhanced BC tumor growth and lipid metabolism *in vivo*.

Ubiquitination is the key to protein posttranslational modification and plays an indispensable role in the mediation of protein stability [38]. Ubiquitination is tightly associated with cancer initiation, development, and even metastasis [39]. As an E3 ubiquitin ligase, NEDD4L has been indicated to catalyze ubiquitination of Yes1-associated transcriptional regulator (YAP1) in BC [40]. Through the research of protein interaction, we found there was a significant interaction between NEDD4L and RHOF. As for the effect of NEDD4L on RHOF, it was observed that NEDD4L reduced the protein stability of RHOF and increased the ubiquitination level of RHOF. In consistent with the previous studies, NEDD4L could inhibit RHOF expression via ubiquitination-mediated degradation of RHOF. Then, we found the reverse of RHOF for the function of NEDD4L in BC cells, elucidating that NEDD4L impeded cell progression through driving ubiquitination and degrading RHOF in BC. The research of NEDD4L in lipid metabolism is few. Cellular lipid peroxidation levels in oesophageal squamous cell carcinoma were enhanced by NEDD4L [23] and it exhibited the expression regulation on lipid metabolism-associated CRTC3 [24], implicating the potential involvement of NEDD4L in regulating lipid metabolism. Herein, NEDD4L reduced the levels of lipids (triglyceride, cholesterol, phospholipid) and related proteins (FASN, SREBP1) by targeting RHOF, validating that the NEDD4L/RHOF axis blocked the lipid metabolism of BC cells.

In recent years, m6A methylation modification has emerged as central contributors to the biological processes of cancers [41]. ALKBH5 is a demethylase with an essential role in a range of human cancers, by mediating the expression of downstream targets. Hu *et al*. testified that ALKBH5 repressed gastric cancer cell invasion by leading to the expression change of protein kinase, membrane-associated tyrosine/threonine 1 (PKMYT1) via the m6A methylation [42]. In colorectal cancer, ALKBH5 aroused immune suppression through m6A modification of Axis inhibition protein 2 (AXIN2) [43]. We found that NEDD4L had m6A modification sites and predicted the binding of ALKBH5 and NEDD4L. ALKBH5 could reduce NEDD4L expression and m6A level of NEDD4L, which implicated that NEDD4L was down-regulated by ALKBH5 in an m6A-dependent manner. However, there are still some limitations in the current conditions. We only explored the interaction relation between ALKBH5 and NEDD4L, while the functional analyses of ALKBH5/NEDD4L in BC cells are lacking. In addition to this, whether ALKBH5 is associated with RHOF is completely undisclosed. These issues will provide the direction for our further research.

In conclusion, NEDD4L knockdown contributed to cell malignant behaviors (increased proliferation, migration, invasion, and reduced apoptosis) and lipid metabolism of BC via inhibiting ubiquitination-mediated RHOF degradation, and NEDD4L was down-regulated by ALKBH5 in an m6A-dependent way. NEDD4L/RHOF axis was first uncovered as a novel molecular mechanism targeting cell progression and lipid metabolism. NEDD4L might be useful in the targeted therapies of BC.

CRediT authorship contribution statement

Tao Liu: Resources, Supervision, Formal analysis, Writing – original draft, Project administration. **Xiaoming Lin:** Software, Data curation, Formal analysis, Methodology. **Rong Liang:** Visualization, Writing – review & editing, Conceptualization, Investigation.

Financial support

This research did not receive any specific grant from funding agencies in the public, commercial, or not-for-profit sectors.

Declaration of competing interest

The authors declare that they have no known competing financial interests or personal relationships that could have appeared to influence the work reported in this paper.

Supplementary material

https://doi.org/10.1016/j.ejbt.2025.07.001.

Data availability

Data will be made available on request.

References

[1] Katsura C, Ogunmwonyi I, Kankam HK, Saha S. Breast cancer: Presentation, investigation and management. Br J Hosp Med 2022;83(2):1–7. https://doi.org/10.12968/hmed.2021.0459. PMid: 35243878.

[2] Sadeghi M, Cava C, Moisavi P, et al. Construction of prognostic ceRNA network landscape in breast cancer to explore impacting genes on drug response by integrative bioinformatics analysis. Lett Drug Design Discov 2024;21(12):2467–81. https://doi.org/10.2174/0115701808255183230922110002.

[3] Bray F, Laversanne M, Sung H, et al. Global cancer statistics 2022: Globocan estimates of incidence and mortality worldwide for 36 cancers in 185 countries. CA Cancer J Clin 2024;74(3):229–63. https://doi.org/10.3322/caac.21834. PMid: 38572751.

[4] Rossi L, Mazzara C, Pagani O. Diagnosis and treatment of breast cancer in young women. Curr Treat Options Oncol 2019;20(12):86. https://doi.org/10.1007/s11864-019-0685-7. PMid: 31776799.

[5] Loibl S, Poortmans P, Morrow M, et al. Breast cancer. Lancet 2021;397(10286):1750–69. https://doi.org/10.1016/S0140-6736(20)32381-3. PMid: 33812473.

[6] Xiong X, Zheng LW, Ding Y, et al. Breast cancer: Pathogenesis and treatments. Signal Transduct Target Ther 2025;10(1):49. https://doi.org/10.1038/s41392-024-02108-4. PMid: 39966355.

[7] Rusnáková DS, Aziri R, Dubovan P, et al. Detection, significance and potential utility of circulating tumor cells in clinical practice in breast cancer. Oncol Lett 2025;29(1):10. https://doi.org/10.3892/ol.2024.14756. PMid: 39492933.

[8] Mosaddeghzadeh N, Ahmadian MR. The RHO family GTPases: Mechanisms of regulation and signaling. Cells 2021;10(7):1831. https://doi.org/10.3390/cells10071831. PMid: 34359999.

[9] Crosas-Molist E, Samain R, Kohlhammer L, et al. RHO GTPase signaling in cancer progression and dissemination. Physiol Rev 2022;102(1):455–510. https://doi.org/10.1152/physrev.00045.2020. PMid: 34541899.

[10] Zhao R, Yi Y, Liu H, et al. RHOF promotes Snail1 lactylation by enhancing PKM2-mediated glycolysis to induce pancreatic cancer cell endothelial-mesenchymal transition. Cancer Metab 2024;12(1):32. https://doi.org/10.1186/s40170-024-00362-2. PMid: 39462429.

[11] Yang RM, Zhan M, Xu SW, et al. miR-3656 expression enhances the chemosensitivity of pancreatic cancer to gemcitabine through modulation of the RHOF/EMT axis. Cell Death Dis 2017;8(10):e3129. https://doi.org/10.1038/cddis.2017.530. PMid: 29048402.

[12] Wen X, Li P, Ma Y, et al. RHOF activation of AKT/β-catenin signaling pathway drives acute myeloid leukemia progression and chemotherapy resistance. iScience 2024;27(7):110221. https://doi.org/10.1016/j.isci.2024.110221. PMid: 39021805.

[13] Luo J, Chen S, Chen J, et al. Identification and validation of DNA methylation markers to predict axillary lymph node metastasis of breast cancer. PLoS One 2022;17(12):e0278270. https://doi.org/10.1371/journal.pone.0278270. PMid: 36454866.

[14] Zhang M, Zhang Z, Tian X, et al. NEDD4L in human tumors: Regulatory mechanisms and dual effects on anti-tumor and pro-tumor. Front Pharmacol 2023;14:1291773. https://doi.org/10.3389/fphar.2023.1291773. PMid: 38027016.

[15] Dong H, Zhu L, Sun J, et al. Pan-cancer analysis of NEDD4L and its tumor suppressor effects in clear cell renal cell carcinoma. J Cancer 2021;12(20):6242–53. https://doi.org/10.7150/jca.58004. PMid: 34539897.

[16] Shi Y, Fang N, Wu Y, et al. NEDD4L mediates ITGB4 ubiquitination and degradation to suppress esophageal carcinoma progression. Cell Commun Signal 2024;22(1):302. https://doi.org/10.1186/s12964-024-01685-9. PMid: 38831335.

[17] Guarnieri AL, Towers CG, Drasin DJ, et al. The miR-106b-25 cluster mediates breast tumor initiation through activation of NOTCH1 via direct repression of NEDD4l. Oncogene 2018;37(28):3879–93. https://doi.org/10.1038/s41388-018-0239-7. PMid: 29662198.

[18] Liu L, Zhang C, Qu S, et al. ESR1 inhibits ionizing radiation-induced ferroptosis in breast cancer cells via the NEDD4L/CD71 pathway. Arch Biochem Biophys 2022;725:109299. https://doi.org/10.1016/j.abb.2022.109299. PMid: 35613689.

[19] Zhang G, Cheng C, Wang X, et al. *N6*-Methyladenosine methylation modification in breast cancer: Current insights. J Transl Med 2024;22(1):971. https://doi.org/10.1186/s12967-024-05771-x. PMid: 39468547.

[20] Han X, Ren C, Jiang A, et al. Arginine methylation of ALKBH5 by PRMT6 promotes breast tumorigenesis via LDHA-mediated glycolysis. Front Med 2024;18(2):344–56. https://doi.org/10.1007/s11684-023-1028-4. PMid: 38466502.

[21] Lyu Y, Wang Y, Ding H, et al. Hypoxia-induced m6A demethylase ALKBH5 promotes ovarian cancer tumorigenicity by decreasing methylation of the lncRNA RMRP. Am J Cancer Res 2023;13(9):4179–91. PMid: 37818080.

[22] Bian X, Liu R, Meng Y, et al. Lipid metabolism and cancer. J Exp Med 2021;218(1):e20201606. https://doi.org/10.1084/jem.20201606. PMid: 33601415.

[23] Chen J, Ying K, Sun J, et al. NEDD4l affects KLF5 stability through ubiquitination to control ferroptosis and radiotherapy resistance in oesophageal squamous cell carcinoma. J Cell Mol Med 2024;28(18):e70062. https://doi.org/10.1111/jcmm.70062. PMid: 39317954.

[24] Kim YH, Yoo H, Hong AR, et al. NEDD4L limits camp signaling through ubiquitination of CREB-regulated transcription coactivator 3. FASEB J 2018;32(7):4053–62. https://doi.org/10.1096/fj.201701406R. PMid: 29505301.

[25] Li Z, Wei H, Li S, et al. The role of progesterone receptors in breast cancer. Drug Des Devel Ther 2022;16:305–14. https://doi.org/10.2147/DDDT.S336643. PMid: 35115765.

[26] Zhao H, Liang Y, Sun C, et al. Dihydrotanshinone I inhibits the lung metastasis of breast cancer by suppressing neutrophil extracellular traps formation. Int J Mol Sci 2022;23(23):1510. https://doi.org/10.3390/ijms232315180. PMid: 36499502.

[27] Zeng L, Zhou G, Yang W, et al. Guidelines for the diagnosis and treatment of knee osteoarthritis with integrative medicine based on traditional Chinese medicine. Front Med 2023;10:1260943. https://doi.org/10.3389/fmed.2023.1260943. PMid: 37915321.

[28] Aranda-Rivera AK, Cruz-Gregorio A, Aparicio-Trejo OE, et al. Sulforaphane protects against unilateral ureteral obstruction-induced renal damage in rats by alleviating mitochondrial and lipid metabolism impairment. Antioxidants 2022;11(10):1854. https://doi.org/10.3390/antiox11101854. PMid: 36290577.

[29] Shaverdashvili K, Padlo J, Weinblatt D, et al. KLF4 activates NFκB signaling and esophageal epithelial inflammation via the Rho-related GTP-binding protein RHOF. PLoS One 2019;14(4):e0215746. https://doi.org/10.1371/journal.pone.0215746. PMid: 30998758.

[30] Yin X, Xu R, Song J, et al. Lipid metabolism in pancreatic cancer: Emerging roles and potential targets. Cancer Commun 2022;42(12):1234–56. https://doi.org/10.1002/cac2.12360. PMid: 36107801.

[31] Broadfield LA, Pane AA, Talebi A, et al. Lipid metabolism in cancer: New perspectives and emerging mechanisms. Dev Cell 2021;56(10):1363–93. https://doi.org/10.1016/j.devcel.2021.04.013. PMid: 33945792.

[32] Corn KC, Windham MA, Rafat M. Lipids in the tumor microenvironment: From cancer progression to treatment. Prog Lipid Res 2020;80:101055. https://doi.org/10.1016/j.plipres.2020.101055. PMid: 32791170.

[33] Xiang Y, Miao H. Lipid metabolism in tumor-associated macrophages. In: Li Y, editor. Lipid metabolism in tumor immunity. Advances in experimental medicine and biology. Singapore: Springer; 2021. p. 87–101. https://doi.org/10.1007/978-981-33-6785-2_6. PMid: 33740245.

[34] Zhang R, Chen J, Wang S, et al. Ferroptosis in cancer progression. Cells 2023;12(14):1820. https://doi.org/10.3390/cells12141820. PMid: 37508485.

[35] Fhu CW, Ali A. Fatty acid synthase: An emerging target in cancer. Molecules 2020;25(17):3935. https://doi.org/10.3390/molecules25173935. PMid: 32872164.

[36] Menendez JA, Lupu R. Fatty acid synthase: A druggable driver of breast cancer brain metastasis. Expert Opin Ther Targets 2022;26(5):427–44. https://doi.org/10.1080/14728222.2022.2077189. PMid: 35545806.

[37] He Y, Qi S, Chen L, et al. The roles and mechanisms of SREBP1 in cancer development and drug response. Genes Dis 2024;11(4):100987. https://doi.org/10.1016/j.gendis.2023.04.022. PMid: 38560498.

[38] Liu F, Chen J, Li K, et al. Ubiquitination and deubiquitination in cancer: From mechanisms to novel therapeutic approaches. Mol Cancer 2024;23(1):148. https://doi.org/10.1186/s12943-024-02046-3. PMid: 39048965.

[39] Dewson G, Eichhorn PJA, Komander D. Deubiquitinases in cancer. Nat Rev Cancer 2023;23(12):842–62. https://doi.org/10.1038/s41568-023-00633-y. PMid: 37935888.

[40] Guo Y, Cui Y, Li Y, et al. Cytoplasmic YAP1-mediated ESCRT-III assembly promotes autophagic cell death and is ubiquitinated by NEDD4L in breast cancer. Cancer Commun 2023;43(5):582–612. https://doi.org/10.1002/cac2.12417. PMid: 37005481.

[41] Singh S, Gupta S, Abhishek R, et al. Regulation of m^6A (N^6-Methyladenosine) methylation modifiers in solid cancers. Funct Integr Genom 2024;24(6):193. https://doi.org/10.1007/s10142-024-01467-z. PMid: 39438339.

[42] Hu Y, Gong C, Li Z, et al. Demethylase ALKBH5 suppresses invasion of gastric cancer via PKMYT1 m6a modification. Mol Cancer 2022;21(1):34. https://doi.org/10.1186/s12943-022-01522-y. PMid: 35114989.

[43] Zhai J, Chen H, Wong CC, et al. ALKBH5 drives immune suppression via targeting AXIN2 to promote colorectal cancer and is a target for boosting immunotherapy. Gastroenterology 2023;165(2):445–62. https://doi.org/10.1053/j.gastro.2023.04.032. PMid: 37169182.